2110 *Biochemistry* **2010,** *49,* 2110–2120
DOI: 10.1021/bi902099u

BIOCHEMISTRY
including biophysical chemistry & molecular biology
Article

Structural Features of Intra- and Intermolecular G-Quadruplexes Derived from Telomeric Repeats[†]

Viktor Víglaský,* Luboš Bauer, and Katarína Tlučková

Department of Biochemistry, Institute of Chemistry, Faculty of Sciences, P. J. Safarik University, 04154 Kosice, Slovakia

Received December 7, 2009; Revised Manuscript Received January 24, 2010

ABSTRACT: The 3′ strand of telomeres is composed of tandem repeats of short G-rich sequences which protrude as single-stranded DNA overhangs. These repeats are G_3T_2A in humans and G_4T_2 and G_4T_4 in the ciliates *Tetrahymena* and *Oxytricha*, respectively. We analyzed different quadruplex-forming sequences derived from telomeric sequences, $G_{3+k}(T_{n+k}G_{3+k})_3$ and $G_{3+k}(T_2AG_{3+k})_3$, in the presence of Li^+, Na^+, and K^+ through the use of circular dichroism, UV spectroscopy, and electrophoresis, where $k = 0$ or 1 and $n = 1-3$. Results obtained under the given conditions can provide more detailed information about the quadruplex structure. The major findings are as follows. (i) G-Repeats in solution form a mix of topologically different structures; only $G_3(T_2G_3)_3$ and $G_3(TG_3)_3$ repeats preferentially form the parallel interstrand structure. (ii) The *Tetrahymena* repeat can form at least two intramolecular conformers with different strand orientations and levels of stability. (iii) G-Quadruplex conformation and molecularity strongly depend on the type and concentration of ions used in the solution. The formation of intramolecular quadruplexes is governed by the length of the loops connecting G-runs. Intermolecular G-quadruplex forms are more likely to form in a higher concentration of ions for sequences where G-runs are separated by only one or two nucleotides.

Nucleic acid sequences containing several short runs of guanine nucleotides can form complex higher-order structures, termed quadruplexes. These noncanonical DNA motifs are believed to be involved in a variety of biological functions; it is suggested that they may also be important causal factors in cell aging and human diseases such as cancer (*1*, *2*). There is also evidence that telomeres serve as a type of biological clock, as the telomere structures appear to become shorter with each successive cell cycle. In immortalized cells and in cancer cells, however, telomerase is activated to maintain the length of the telomere (*3*).

The presence of several tracts containing guanines can favor the formation of topologically diverse G-quadruplex structures. The conformational plasticity of DNA depends on the environment (buffer, pH, temperature, etc.) and on the DNA sequence itself (*4*). The formation of G-quartets and their subsequent stacking are fundamental to quadruplex formation and stability. Intramolecular quadruplexes form stable structures, especially in the presence of potassium, though small changes in the sequence can have significant effects on the structure and stability (*5*). However, multimolecular conformers are also formed under the same conditions. G-Rich sequences with the ability to form quadruplex structures are found in telomeric regions of DNA, which contain repeated sequences such as $(G_3T_2A)_n$ in humans and most other higher eukaryotes (*6*−*8*), $(G_4T_2)_n$ in *Tetrahymena*, and $(G_4T_4)_n$ in *Oxytricha* and *Stylonchia* (*9*).

Guo et al. studied the stability of the tetramolecular structures formed by $d(T_nG_4)$, where $n = 1-8$, the result being that the most stable structure was formed by the $n = 1$ sequence (*10*). In a study undertaken by Hazel et al., they determined that the length of the loop region of the sequence can have an impact on the folding of G-quadruplexes (*11*). Intermolecular quadruplexes usually adopt a structure in which all the strands are parallel, while the arrangement in intramolecular complexes can be parallel, antiparallel, or a combination of both (*12*).

However, there is still some debate over which structure is biologically relevant (*13*). The NMR[1] structure of a four-repeat human telomeric sequence $[d(T_2AG_3)_4]$ was shown to be a folded antiparallel monomolecular G-quadruplex in the presence of Na^+ (*14*). In contrast, the resolved crystal structure of the same sequence in the presence of K^+ showed that the G-quadruplex is indeed monomolecular, but that it is an all-parallel-stranded structure with all loops being of the propeller type (*15*). This structure does not seem to be a prevalent form in solution (*12*, *16*). Different conformations of human telomeric oligomers in water solutions and in crystals have been reported by several authors (*13*, *14*). Instead, the structure adopted in the presence of K^+ is a mixture of two hybrid structures comprised of three parallel strands and a fourth pointing in the opposing direction (*17*, *18*). Several recent studies have shown that sequences closely related to the human telomeric repeat adopt a mixed topology with one double-chain reversal and two edgewise loops (*16*, *19*, *20*).

Several spectroscopic techniques can be used to monitor the structural stability of G-quadruplexes: UV molecular absorption,

[†]This study was supported by grants from the Slovak Grant Agency (1/0053/08 and 1/0153/09).

*To whom correspondence should be addressed: Safarik University, Faculty of Sciences, Institute of Chemistry, Department of Biochemistry, Moyzesova 11, 04011 Kosice, Slovakia. Telephone: +421 55 234 12 62. Fax: +421 55 622 21 24. E-mail: viktor.viglasky@upjs.sk.

[1]Abbreviations: TGGE, temperature-gradient gel electrophoresis; TBA, thrombin binding aptamer; NMR, nuclear magnetic resonance.

 Published on Web 02/10/2010

Table 1: Oligodeoxynucleotides Used in This Study

name	no. of nucleotides	ε^a (mM^{-1} cm^{-1})	sequence[b] (5′ → 3′)
G3T	15	170.4	GGGTGGGTGGGTGGG
G3T2	18	199.2	GGGTTGGGTTGGGTTGGG
G3T2A	21	245.4	GGGTTAGGGTTAGGGTTAGGG
G3T3	21	228.0	GGGTTTGGGTTTGGGTTTGGG
G4T2	22	246.4	GGGGTTGGGGTTGGGGTTGGGG
G4T2A	25	292.6	GGGGTTAGGGGTTAGGGGTTAGGGG
G4T3	25	275.2	GGGGTTTGGGGTTTGGGGTTTGGGG
G4T4	28	304.0	GGGGTTTTGGGGTTTTGGGGTTTTGGGG
20mer	20	−	GCTATGGCTTGCTATGGCTT
40mer	40	−	GCTATGGCTTGCTATGGCTTGCTATGGCTTGCTATGGCTT

[a]Millimolar extinction coefficient. [b]G-Runs are underlined.

circular dichroism (CD), fluorescence (FRET), and NMR. Of these methods, UV/CD can be considered the most appropriate technique, because the measured instrumental response is extremely sensitive to the distance between the interacting strands, and the inclination and the distance between the bases and the axis of the structure; the technique can also be performed with acceptable costs. Electrophoresis is another commonly used technique. During electrophoretic separation, the samples of negatively charged DNA fold into various structures and they move toward the anode at different rates.

In this article, the effects of systematically varying G-tracts and the loop lengths of the four repeats derived from telomeric sequences are evaluated by CD and polyacrylamide gel electrophoresis (PAGE). We not only focus on biologically relevant sequences but also analyze a wider range of quadruplex-forming sequences, $d[G_{3+k}(T_{n+k}G_{3+k})_3]$ and $d[G_{3+k}(T_2AG_{3+k})_3]$, where $k = 0$ or 1 and $n = 1-3$, as they can offer valuable information about quadruplex folding. All of these sequences, where $k = 0$, occur in the human genome in many copies. In addition, comparative thermodynamic analysis in the presence of three different monovalent ions is also performed.

MATERIALS AND METHODS

Material and Equipment. All chemicals and reagents were obtained from commercial sources. The acrylamide/bisacrylamide (19:1) solution and ammonium persulfate were purchased from Bio-Rad, and polyethylene glycol (PEG) 200 and *N*,*N*,*N*′,*N*′-tetramethylethylenediamine were purchased from Fisher Slovakia. DNA oligomers (sequences listed in Table 1) were obtained from Sigma Genosys and Biosearch Technologies, Inc. All DNA oligomers were PAGE-purified and dissolved in doubly distilled water before use. Single-strand concentrations were precisely determined by measuring the absorbance (260 nm) at 90 °C using molar extinction coefficients provided by Sigma Genosys. The concentration of DNA was determined by UV measurements taken with a Varian Cary 100 UV−visible spectrophotometer (Amedis). Cells with optical path lengths of 10 mm were used, and the temperature of the cell holder was controlled with an external circulating water bath (Varian).

Circular Dichroism Spectroscopy. CD spectra were recorded on a Jasco (Easton, MD) J-810 spectropolarimeter equipped with a PTC-423 L temperature controller using a quartz cell with an optical path length of 1 mm in a reaction volume of 300 μL and an instrument scanning speed of 100 nm/min, a 1 nm pitch, and a 1 nm bandwidth, with a response time of 2 s, over a wavelength range of 220−320 nm. The scan of the buffer was subtracted from the average scan for each sample. CD spectra were collected in units of molar circular dichroism versus wavelength. The cell holding chamber was flushed with a constant stream of dry nitrogen gas to prevent the condensation of water on the cell exterior. All DNA samples were dissolved and diluted in suitable buffers containing appropriate concentrations of ions. The concentration of DNA oligomers used in the experiment was kept close to ∼2.5 μM; absorbances were chosen to give an absorption of ∼0.4−0.8 at the absorption maximum. Circular dichroism was expressed as the difference in the molar absorption of the right-handed and left-handed circularly polarized light, $\Delta\varepsilon$, in units of M^{-1} cm^{-1}. The molarity was related to DNA oligomers; the final spectra express the same DNA strand concentration of oligomer which is essential for accurate CD amplitude information. DNA samples were annealed at 95−98 °C for 5 min and then allowed to cool for ∼2 h to the initial temperature at which the samples were kept at the beginning of the experiment. CD data represent three averaged scans taken over a temperature range from 20 to 95 °C and for less stable structures a range from −5 to 80 °C. All CD spectra are baseline-corrected for signal contributions caused by the buffer. The Britton-Robinson buffer was used in all experiments: 25 mM H_3PO_4, 25 mM boric acid, and 25 mM acetic acid supplemented with appropriate concentrations of KCl, NaCl, and LiCl. The pH was adjusted with Tris to the final value of 7.0.

Melting Curves. The CD melting profiles were recorded at 265 and 295 nm. The thermal stability of different antiparallel quadruplexes was also measured by recording the UV absorbance and the CD ellipticity at 295 nm as a function of temperature, by a method similar to that published previously (*21*). The temperature ranged from 20 to 95−99 °C, and the heating rate was 0.25 °C/min. The melting temperature (T_m) was defined as the temperature of the midtransition point. T_m was estimated from the peak value of the first derivative of the fitted curve. This T_m value was used as an initial parameter of thermodynamic analysis. From the relation $\Delta G^\circ = -RT\ln(K) = \Delta H^\circ - T\Delta S^\circ$, we can deduce that $\ln(K) = -(\Delta H^\circ/R)(1/T) + (\Delta S^\circ/R)$. Thus, $\ln(K)$ can be expressed as a linear function of $1/T$. The equilibrium constant K can be written as $K = \alpha/(1-\alpha)$ for an intramolecular equilibrium (α is the fraction of folded oligodeoxynucleotide). α (in the range of 0−1.0) and K can easily be determined at each temperature from the melting profiles. By assuming a two-state unfolding mechanism, we can calculate the fraction of unfolded molecule, $1-\alpha$, using the equation $1-\alpha = (Y_f - Y_{obs})/(Y_f - Y_u)$, where Y_{obs} is an observed variable parameter (e.g., mobility, absorbance, ellipticity, fluorescence, etc.) and Y_f and Y_u are the values of Y characteristic of the folded

and unfolded conformations, respectively. An evaluation of equilibrium constants in the transition region requires extentions of pre- and postunfolding baselines into the transition region: $Y_f(T) = Y_f(T_0) + A_fT$ and $Y_u(T) = Y_u(T_0) + B_fT$, where $Y_f(T_0)$ and $Y_u(T_0)$ are intercepts and A_f and B_f are slopes of pre- and postunfolding regimes, respectively. Then $\Delta G^\circ = -RT \ln(Y_f - Y_{obs})/(Y_{obs} - Y_u)$ (*21*). From this equation, we can easily express $Y(T) = [Y_f + Y_u \exp(\Delta G/RT)]/[1 + \exp(\Delta G/RT)]$ and then $Y(T) = \{Y_f(T_0) + A_fT + [Y_u(T_0) + B_uT] \exp(\Delta H - T\Delta S/RT)\}/[1 + \exp(\Delta H - T\Delta S/RT)]$, with Y_f, Y_u, A_f, B_u, ΔH, and ΔS as fitting parameters. For a biphasic transition curve, we evaluated each transition separately (Figure S8 of the Supporting Information). The goodness of fit of a statistical model describes how well it fits a set of observations. Therefore, the reduced χ^2 parameter was calculated for each fit. When the deviation is greater than 5%, the fitting curve does not describe two-state unfolding.

Electrophoresis. Native polyacrylamide gel electrophoresis (PAGE) was conducted in a temperature-controlled vertical electrophoretic apparatus (Z375039-1EA, Sigma-Aldrich, San Francisco, CA). The gel concentration was 16% (19:1 monomer: bis ratio, Applichem, Darmstadt, Germany). Approximately two micrograms ($^1/_5$ of the amount of DNA that was used for CD experiments) was loaded on 14 cm × 16 cm × 0.1 cm gels. Electrophoreses were run at 10, 20, and 55 °C for 4 h at 126 V (~8 V cm^{-1}). A description of the TGGE equipment used has been published previously (*22*). However, for this kind of experiment, ~10−15 μg of DNA was loaded into the electrophoretic well. DNA oligomers were visualized with silver after the electrophoresis, and the electrophoretic record was photographed with an Olympus Camedia 3000 camera (*23*). Objective melting curves from electrophoresis were obtained using the procedure that has been described previously (*22*).

RESULTS

We recorded the CD spectra, PAGE, and thermal melting profiles of a series of oligonucleotides that contain G-tracts of varying lengths, specifically, three and four guanines. G-Tracts in series are separated by bases, which can form loops of quadruplex structures with lengths between one and four: T, TT, TTT, TTA, and TTTT (Table 1).

CD Spectroscopy of G-Rich Oligonucleotides. The CD spectra of quadruplexes can be used to indicate whether they fold into a parallel or antiparallel configuration (*16*). Quartet stacking and the polarity of DNA strands are the determining factors of the intensity and shape of the CD spectrum, in particular the rotation angle between the stacks (*20*, *24*). However, the interpretation of optical properties such as hypochromicity or the shape and sign of CD bands can be controversial (*25*). Antiparallel quadruplexes exhibit positive CD signals at ~295 nm, with a negative signal at 260 nm, and in addition the 3+1 conformer exhibits a shoulder at 265−270 nm (*18*). In contrast, parallel G-quadruplex structures give a positive band at ~265 nm and a negative peak at 240 nm. Unfolded oligonucleotides do not display these spectral signatures. These spectral features are mainly attributed to the specific guanine stacking in various G-quadruplex structures (*26*, *27*). Figure 1 shows CD spectra of oligonucleotides in Britton-Robinson buffer containing 50 mM KCl, NaCl, and LiCl. In addition, CD measurements were performed in the same buffer containing 0, 2.5, 25, and 200 mM KCl at pH 7.0. Before the CD measurements, each DNA sample was dissolved in an appropriate buffer, heated to 95−98 °C, and slowly cooled to the initial temperature of the CD/UV measurement. One can see that, in the presence of K^+ and Na^+, only the G_3T and G_3T_2 sequences display a major positive peak at ~265 nm with a minimum at ~240 nm, which is typical for a parallel strand arrangement. However, all sequences except G_3T show significant peaks at ~295 nm due to the formation of antiparallel G-quadruplexes in the presence of lithium. G_3T_2 exhibits a slight ellipicity at ~295 nm with a potassium concentration of 25−200 mM, but at 2.5 mM KCl, this peak is more evident. The positive peak at ~295 nm achieves a maximum of ~6−8 M^{-1} cm^{-1} for any sequence in which antiparallel arrangements of G-quadruplexes exist. The molar concentrations of the DNA oligomer are the same for all sequences. The oligonucleotide concentration was determined from the absorbance of oligomers in linearized unfolded states measured under postdenaturing conditions (~95 °C). Each panel in Figure 1 represents a CD spectrum corresponding to the same molar concentration of the strand in cells.

Once again, the G_4T_2 sequence shows a positive CD peak at ~265 nm and a significant peak at ~295 nm in the presence of K^+. Higher concentrations of K^+ cause the peak to increase and decrease to ~265 and ~295 nm, respectively (Figure 1E, red dashed line). The peak at ~295 nm was observed in the presence of Li^+ and Na^+, but the second benchmark peak was detected below 260 nm, similar to that observed previously in other quadruplex-forming aptamers (*24*). However, it has been emphasized previously that a peak under 260 nm does not necessarily reflect the formation of parallel quadruplexes (*28*). It has also been shown that the unpaired guanines in the loops might also affect the CD spectra (*29*). Other oligomers exhibit a maximum of ellipticity at ~293 nm and a minimum at ~265 nm in the presence of Li^+ and Na^+, suggesting that they could form antiparallel quadruplex structures. Interestingly, the negative peak at ~260 nm within the G_4T_2A sequence is observed only in the presence of potassium ions. The TBA sequence (thrombin binding aptamer) shows similar spectral features under the same conditions, which could suggest the antiparallel chair configuration that has been determined previously (*28*). Quadruplexes which show positive peaks at ~295 nm and shoulders at 265 nm may exhibit structural polymorphism, with a significant fraction adopting both antiparallel and parallel strand arrangements. This spectrum profile can be explained by the spectral convolution of parallel and antiparallel conformers (*27*) and by the formation of so-called 3+1 hybrid structures (*18*, *20*, *25*). Such spectral features can be seen clearly in G_3T_3 and G_3T_2A sequences in the presence of K^+.

An unusually high value of ellipticity at ~265 nm for G_3T and G_3T_2 was also observed, mainly in the presence of K^+. On the basis of the suggestions of other authors and our results, it seems that molecularity and molar ellipticity are closely related and that, consequently, elliptic signals depend on the amount of stacked glycosyl bonds (*27*, *30*). In other words, this means that the elliptic signal at ~265 and ~295 nm could be proportional to the number of stacked glycosyl bonds in the *syn* and *anti* configuration, respectively (*27*). However, such an evaluation cannot be confirmed at present, although the conversion of one conformer to other conformations induced by cation, polyethylene glycol (PEG 200), and ethanol has been studied by many authors (*31*−*34*). Currently, we can only hypothesize and suggest that in certain ranges the CD signal is proportional to the orientation of stacked glycosyl bonds and their concentration

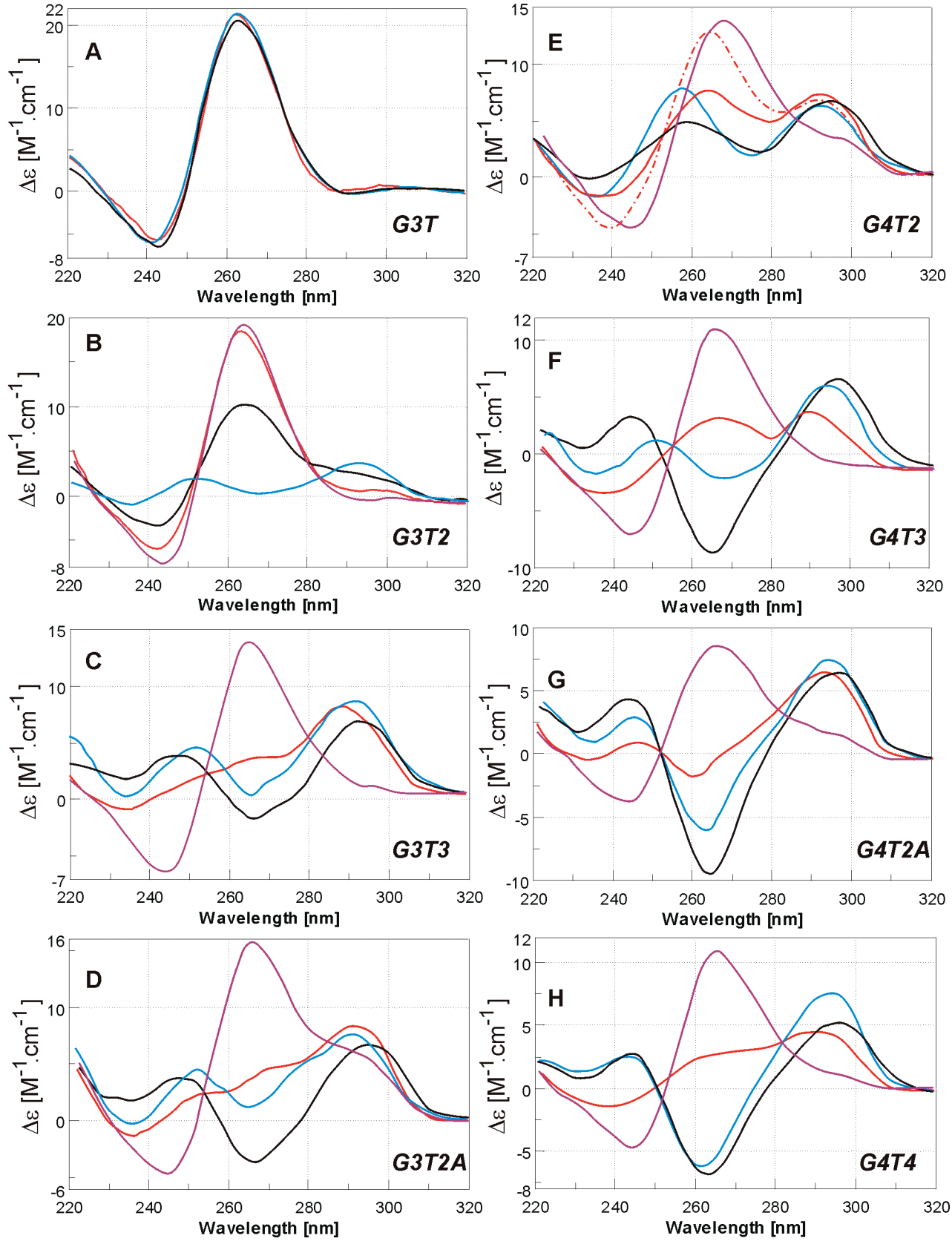

FIGURE 1: CD spectra of $G_{3+k}(T_{n+k}G_{3+k})_3$ and $G_{3+k}(T_2AG_{3+k})_3$ oligonucleotides in 25 mM Britton-Robinson buffer (pH 7.0) in the presence of 50 mM LiCl (blue), NaCl (black), and KCl (red), where $n = 1-3$ and $k = 0$ or 1. In addition, spectra of oligomers in 50 mM KCl and 50% PEG 200 (magenta) are depicted in panels B−H. Each spectrum corresponds to three averaged scans taken at 25 °C and is baseline corrected for the signal contribution caused by the buffer. The dotted−dashed red line in panel e represents the CD spectrum at 200 mM KCl.

in the tetraplex structure (*27*). We are unable to determine the molecularity based on spectra where more than one conformer occurs in solution. Molecularity evaluation can be conducted more precisely when conformers can be compared under separate conditions. In the presence of 50 mM K^+ and 50 mM Li^+, the G_3T_2 oligomers come very close to fulfilling this condition, as

only one positive peak is observed for each, at 263 and 295 nm, respectively. The elliptic signal at 263 nm achieves a value of ~20 M^{-1} cm^{-1} which is ~4 times more than other oligomers achieve at ~295 nm. A similar effect in trombin binding aptamers has been observed (*30*). The detection of an isoelliptic point analogous to an isosbestic point in UV−vis analysis is useful in characterizing the two-state unfolding mechanism (Figures S1 and S2 of the Supporting Information).

In addition, the rates of heating and cooling are determining factors in the formation of different conformers, as is the ratio of ellipticity at 265 and 295 nm. This effect is more significant for G_4X series, mainly for G_4T_2 and G_4T_4 oligomers, where X is T_2, T_3, T_2A, and T_4. After the samples of DNA dissolved in an appropriate buffer containing potassium had been defrosted, significant peaks were observed at 295 nm, but after the sample had been heated and slowly cooled, this peak was reduced in magnitude and the peak at ~265 nm increased in magnitude. When this process was repeated two or three times, only minor changes were detected. However, when the DNA samples were frozen again, after a few days a significant peak at 295 nm was observed after defrosting. The effect of a sample defrosting was repeated multiple times within a few weeks. Here we can clearly see that a small decrease in the magnitude of the CD signal at 295 nm can cause a significantly larger change in the CD signal at 265 nm for the G_4T_2 oligomer (Figure 1E). This suggests that a monomolecular structure converts into a multimolecular one, where an increasing level of stacking G-quartets offers stronger CD signals. Our suggestion would appear to support the electrophoretic analysis. Interestingly, the magnitude of the CD signal at ~265 nm increases after conversion and condition exchange (e.g., ions).

Electrophoretic Analysis. Electrophoretic separation can offer additional information about the molecularity of G-quadruplexes, and the results are presented in Figure 2. We applied a comparison similar to that performed previously using $(G_nT)_4$ and $(G_nT_2)_4$ oligomeric sequences (*29*). The relative mobility of the various folded species is very different in the presence of different ions (Figure 2). The mobilities of the fastest bands of G_3T_3, G_3T_4, G_4T_2, G_4T_3, and G_4T_2A are similar, while G_3T_2A moves even faster in the presence of potassium (Figure 2a). This observation could be explained by the number of potassium ions bonded in each complex, suggesting that they reflect the number of stacked G-quartets in each complex (*29*). However, the mobility of the DNA sample depends on many factors, e.g., conformation, charge, and molecular mass. The intensity of the slowly migrating species also depends on the method of annealing and on the sequence of DNA. We assume that the slowly migrating species correspond to multimeric intermolecular complexes, while the fastest species are intramolecular (*29*, *35*, *36*). Interestingly, G_4T_2 displays two faster well-recognized bands, corresponding to intramolecular conformers, and the next slower band represents the multimeric structure. Both G_3T_2 and G_3T oligomers have mobility levels similar to those of the third slowly migrating band of G_4T_2, but they show peaks at 265 nm and not at 295 nm by CD spectroscopy, which would seem to correspond to a parallel arrangement. The presence of Na^+ again caused the formation of multimeric conformers mainly for G_4X series (Figure 2b). However, the presence of Li^+ caused a larger amount of G_3X and G_4X series to fold into defined monomolecular states (Figure 2c). Although the silver staining procedure is very sensitive to the presence of any other conformational species, the intensity of the band may not be proportional to the molecule

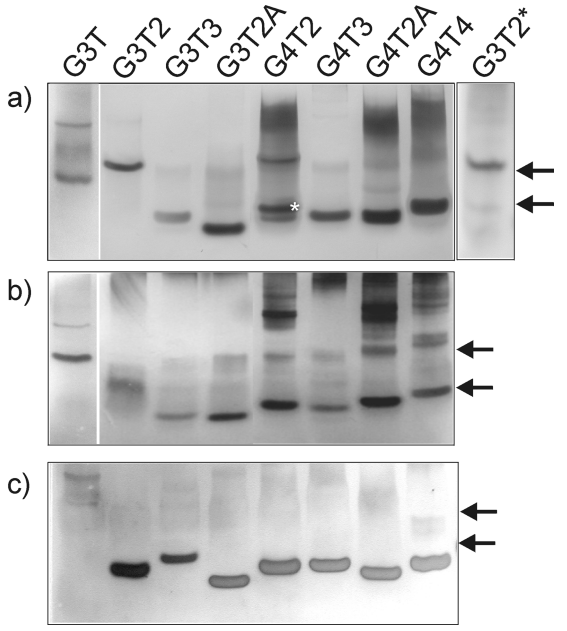

FIGURE 2: Oligonucleotides resolved by gel electrophoresis and visualized by silver staining. Mobility of the oligonucleotides in polyacrylamide gels at 22 °C in 25 mM Britton-Robinson buffer (pH 7.0) containing (a) 50 mM KCl, (b) 50 mM NaCl, and (c) 50 mM LiCl. G_3T, G_3T_2, G_3T_3, G_3T_2A, G_4T_2, G_4T_3, G_4T_2A, and G_4T_4 were loaded in lanes 1−8, respectively. In addition, the electrophoretic record of G_3T_2 at 2.5 mM KCl marked with an asterisk is shown in panel a. The magnitude of the band of G_4T_2 marked with the white asterisk is diminished when electrophoresis is performed at 55 °C (Figure S4 of the Supporting Information). As a control, random oligomers were also loaded (20- and 40mers). Their positions after the electrophoresis are marked by arrows beside each panel. The DNA sample prior to use was heated in the same buffer for 5 min at ~98 °C and slowly cooled to room temperature within 50 min.

concentration. In the Supporting Information, we present the same gel stained twice with the silver procedure, but the second staining shows that no oligomers form only a single conformer in solution, which agrees with the CD spectral measurements (Figure S3 of the Supporting Information). The recent results obtained by mass spectroscopy for a series of similar sequences and conditions have shown that G_3T_2 and G_3T_3 could form only an intramolecular monomer (*37*). The electrospray assay is comparable with the results for which very low concentrations of ions were used (not shown). Therefore, we observe a small discrepancy in these results; the band of G_3T_2 moves significantly more slowly than those of the other monomolecular species (Figure 2a,b). However, the CD results show a positive peak at 265 nm that corresponds to a parallel conformer (Figure 1B). Similar mobility effects have been observed for many other G-rich oligomers predominantly forming parallel quadruplexes: the nuclease hypersensitive promoter elements of *c-myc*, *vegf*, *ret*, and *kras* and the inhibitor of HIV integrase (not shown). There are two possible explanations for G_3T_2 anomalous mobility. (i) It is possible that the parallel topology of the quadruplex, rather than the molecularity, would have a greater influence on the electrophoretic mobility. However, experiments in which various amounts of potassium were used confirm the fact that a small population of fast moving monomolecular species is formed at KCl concentrations of < 2.5 mM (Figure 1A). (ii) The anomalous mobility of G_3T_2 and the corresponding bands of G_4T_2 and G_3T represent a multimeric quadruplex structure; we suggest that it consists of two to four parallel strands. In addition, our suggestion

is supported by the CD spectra where the same amount of DNA oligomer has been used (Figure 1). The CD ratios between the peaks at 265 and 293 nm for the same molar amount of G_3T_2 and G_3T_2A are approximately 2, 3, and 4 at 2.5, 25, and 50−200 mM KCl, respectively. A similar mobility can also be seen within the G3T oligomer, but its melting temperature is higher than 100 °C at a millimolar potassium concentration (*29*, *36*). The mobility of the G_3T_2 oligomer in 50 mM NaCl could correspond to an intramolecular dimer, such as the interlocked dimeric parallel-stranded HIV DNA quadruplex (*38*), but this band is smeared probably because of wobbling conformational states during electrophoresis. In the presence of Li^+, G_3T_2 and G_3T_3 move more slowly than an intramolecular monomer but their mobilities are identical to those of unfolded 18mers and 21mer; here we suggest that these bands might correspond to unfolded linear structures (Figure 2c). In spite of the mobility of G_3T_2 which could also correspond to that of a dimer of G_3T_2, the ellipticity is not twice as high, which would be expected for a dimeric molecule. Thus, in the suggested structure of G_3T consisting of four parallel strands, there are three stacked G-tetrads separated by only one thymine residue in each strand, and in G_3T_2 and G_4T_2, two thymine residues separate a cluster of G-tetrads (Figure 3d−f). The hairpin dimer is excluded because no signal was detected at 295 nm in the CD spectra of G_3T and G_3T_2. Interestingly, TBA shows an elliptic signal at 295 nm at the same molar concentration of ~16 M^{-1} cm^{-1}, what corresponds to that of the hairpin dimer (not shown). A quadruplex structural arrangement of this type would explain their extreme stability. The extreme stability of four-interstrand tetraplexes can be explained by the fact that each quadruplex contains 12 stacked tetrads instead of three as observed in monomolecular structures (Figure 3). Therefore, the order of the stability of a four-strand structure is as follows: $G_3T > G_4T_2 > G_3T_2$ (Figure 4 and Table 2). Three or more unpaired nucleotides between G-runs cause additional destabilization of a four-strand G-quadruplex. The result of this is that the monomolecular intrastrand G-quadruplexes become the more prevalent conformation. They are more thermodynamically stable in solution in the presence of K^+, Na^+, and Li^+ than in intermolecular structures. If the monomolecularly folded tetraplexes formed noninterlocked oligomeric structures, we would observe a ladder of oligomers after electrophoretic separation, but this effect has never been observed. Therefore, we suggest that the interlocked multimeric structure is more likely and more stable than a monomolecular G-quadruplex structure; the four-strand parallel G-quadruplex structure is a marginal case.

The band of G_4T_2 marked with an asterisk disappeared when the electrophoretic separation was performed at 55 °C (Figure S4 of the Supporting Information). Other species are less sensitive to the temperature increase, but G_3T_3 and G_3T_2 show a small population of unfolded structures, because the melting temperature of these oligomers is close to the temperature inside the electrophoretic gel (Table 2 and Figure S4 of the Supporting Information). A higher temperature causes a partial elimination of the intermolecular slowly migrating species.

The oligomers used here typically fold into a mixed parallel/antiparallel topological configuration, although G_3T_2 and G_4T_2 predominantly form a parallel intermolecular conformation in the presence of potassium, but these conformations are mostly intermolecular.

CD and UV Melting Curves of G-Quadruplexes. Curve analysis typically assumes a two-state equilibrium between the folded and unfolded forms; the result is an S-shaped dependence of the melting process. However, the presence of polymorphic quadruplex structures usually leads to a melting profile that deviates from this dependence. Nonsigmoidal shapes of the melting curve have been reviewed by many authors (*39*, *40*). If DNA quadruplexes unfold in a two-state mechanism, then the dependence of the CD signal at two different wavelengths is directly proportional [$CD_{\lambda 2}(T) = K \times CD_{\lambda 1}(T)$] and the isoelliptic (isodichroic) points should be clearly detected. However, our spectra collected during the melting curve measurement show that this is not valid for all sequences (Figures S1 and S2 of the Supporting Information). The detection of isoelliptic points is summarized in Table S1 of the Supporting Information. However, the presence of isoelliptic and isobestic points may not in itself be a sufficient requirement for the two-state melting of one individual topological state, because electrophoresis confirms the presence of more conformers prior to their total denaturation. The van't Hoff analysis of shallower melting profiles often offers smaller apparent values of ΔH (*39*). This effect is most evident in the sequence of G_4T_4 at 50 mM KCl (Figure 4H and Table 2).

In the case of one conformer converting to another more stable conformer, the CD melting curve can initially increase over a certain range of temperatures up to the saturation of the conformational state and then again decrease at ~295 nm, but at ~265 nm, a biphasic transition, two apparent decreases were observed (Figure 4E and Figure S5 of the Supporting Information). The UV melting curve is also biphasic (Figure S5 of the Supporting Information). This nonsigmoidal transition effect is observed in *Tetrahymena* repeats. If this is the case, then each transition must be evaluated separately. Nevertheless, the values obtained from CD and UV melting curves are consistent with those previously determined for intramolecular quadruplexes, where the same methods have been used (*28*, *29*, *41*) (Table 2). The table summarizes average values of CD and UV melting data obtained at 265 and 295 nm and at 295 nm, respectively. If the ellipticity maximum was achieved at 265 (295) nm, then the CD melting curves were obtained at 265 (295) nm. The apparent melting temperatures summarized in Table 2 again clearly demonstrate that the number of G-tetrads in quadruplexes and molecularity are important determining factors in the thermal stability of G-quadruplexes. In addition, the molecularity of G-quadruplexes is also closely related to the type of monovalent ion. Previously published data showed that it is difficult to find a simple correlation between the loop length and thermodynamic stability of quadruplexes, in contrast to the correlation documented for model sequences (*42*).

TGGE of G-Quadruplexes. TGGE can help to solve the problem of quadruplex polymorphism, because electrophoresis allows us to distinguish between different conformers and evaluate the most abundant conformers. TGGE offers an objective melting profile over a temperature gradient (*22*). The results depicted in Figure 5 clearly demonstrate that the number of nucleotides between G-runs in quadruplexes is the determining factor for the thermal stability of both intramolecular and intermolecular G-quadruplexes. However, to capture the whole pre- and postmelting regimes of the quadrupex transition, only 2.5−25 mM KCl could be used, because the temperature range of the TGGE experiment is limited to a maximum of 80 °C. The basis of this experiment was the fact that a decreasing concentration of potassium causes the destabilization of G-quadruplex structure (*37*, *43*). The obtained results can be

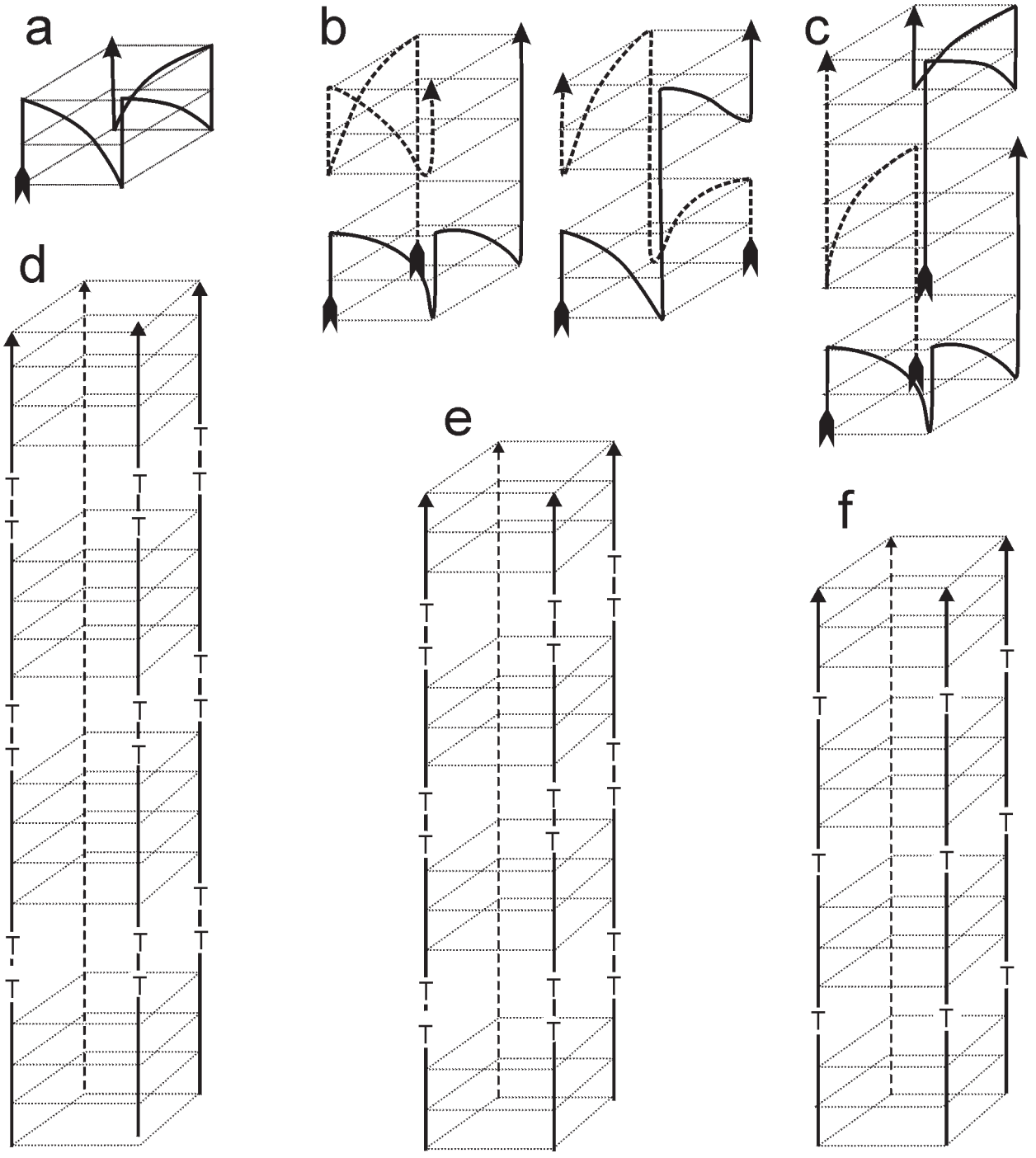

FIGURE 3: Schematic drawing of possible G-quadruplex parallel structures: parallel (a), interlocked dimer (b), interlocked trimer (c), and four-strand structures of G_4T_2 (d), G_3T_2 (e), and G_3T (f).

extrapolated to a higher concentration of potassium in solution. Despite the low concentration of potassium, the melting transition and the postdenaturing state of G_3T and G_4T_2A are out of the TGGE range. Nevertheless, the TGGE results elucidate and confirm many of the crucial suggestions described above. The thermal stability of intramolecular monomers in the presence of 50 mM potassium is as follows: $G_3T_3 \leq G_4T_3 < G_3T_2A < G_4T_2 \leq G_4T_2A < G_4T_4$ (Figure 5A,D and Table 2). These results are in agreement with the spectral data. Additionally, the TGGE results again confirm that not only the concentration but also the type of ion is the determining factor in the thermal stability of G-quadruplexes. Potassium ions can stabilize the G-quadruplex structure more effectively than sodium ions (Figure 5A,B and Table 2). However, for four-strand parallel G-quadruplexes, the thermal stability increases in the following order: $G_4T_2 < G_3T_2 < G_3T$ (Figure 5C,D). The more preferred form of G_4T_2 at 2.5 mM KCl is the intramolecular antiparallel conformation, but a larger amount of potassium facilitates the formation of multimeric parallel conformers (Figures 2a and Figure 3c,d). The melting profile of the corresponding bands in Figure 2a is very similar to that of the G_3T_2 oligomer.

It is important to note that spectral measurements of any type, and also microcalorimetry, do not always allow us to distinguish between conformers occurring in solution. This means that for a mixed population of conformers in any sequence, TGGE can offer more relevant results.

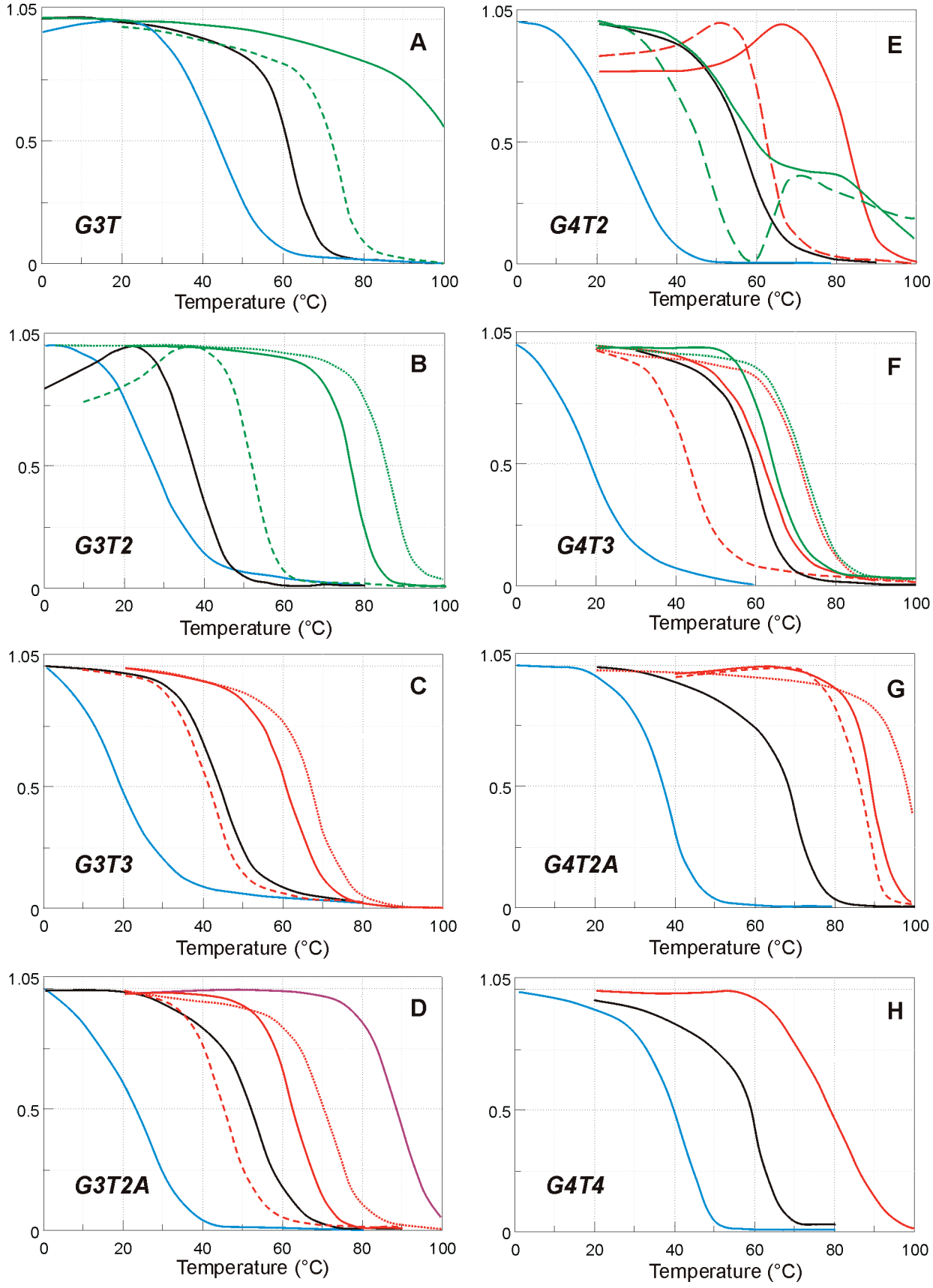

FIGURE 4: Normalized CD melting curves of $(G_{3+k}T_{n+k})_3G_{3+k}$ and $(G_{3+k}T_2A)_3G_{3+k}$ oligonucleotides in 25 mM Britton-Robinson buffer (pH 7.0) in the presence of 50 mM LiCl (blue), NaCl (black), and 2.5 mM KCl (red and green dashed lines), 50 mM KCl (red and green solid lines), or 200 mM KCl (red and green dotted lines), where $n = 1-3$ and $k = 0$ or 1. Red and green lines represent measurements at 293 and 263 nm, respectively. In addition, the CD melting curve of the G_3T_2A oligomer at 263 nm in 50 mM KCl and 50% PEG 200 (magenta) is depicted in panel D. Melting curves were collected by CD spectroscopy at 265 and 295 nm for parallel (P) and antiparallel (A) structures, respectively. UV melting curves were determined at 295 nm. The values of thermodynamic parameter ΔH of the individual tetraplexes were determined from the melting curves generated by monitoring at 295 nm.

Table 2: Apparent Melting Temperatures of G-Quadruplexes of UV and CD Melting Curves Shown in Figure 4[a]

		50 mM LiCl		50 mM NaCl		2.5 mM KCl		50 mM KCl		200 mM KCl	
oligo	form[b]	T_m (°C)	ΔH_{vH} (kcal/mol)	T_m (°C)	ΔH_{vH} (kcal/mol)	T_m (°C)	ΔH_{vH} (kcal/mol)	T_m (°C)	ΔH_{vH} (kcal/mol)	T_m (°C)	ΔH_{vH} (kcal/mol)
G_3T	P	39.9	32.0/42.1	62.4	70.0/75.7	73.9	73.2	>100	–	>100	–
G_3T_2	P	–	–	35.6	42.6	49.9	64.8	77.4	72.2	86.5	68.2
	A	25.8	28.6/27.8	–	–	–	–	–	–	–	–
	E	–	–	–	–	50.5	67.7	–	–	–	–
G_3T_2A	A	25.2	31.9/23.2	53.7	44.4/50.4	46.1	46.6/45.7	63.4	46.9/42.7	72.2	44.5/43.6
	P[c]	–	–	–	–	–	–	89.9	59.1	–	–
	E	–	–	54.1	45.1	–	–	63.7	47.2	–	–
G_3T_3	A	18.3	29.0/26.9	43.9	39.8/40.2	41.3	48.7/42.9	61.9	50.5/52.1	68.8	53.7/49.5
	P[c]	–				–	–	86.7	63.3		
G_4T_2	A	28.6	20.7/17.2	57.4	48.0/45.0	61.9	71.2/70.9	83.1[d]	71.6[d]	BC	BC
	P	–	–	–	–	–	–	–	BC	94.5[d]	–
	E	–	–	56.2	49.4	62.1	66.6	–	–	–	–
G_4T_2A	A	39.3	38.8/40.0	70.4	69.8	69.8	73.4/71.2	90.4	66.9	~99	–
G_4T_3	A	20.5	28.0/25.9	60.5	62.4/59.2	42.8	51.1/42.3	63.3	49.5/44.9	72.6	56.8/55.3
	P	–	–	–	–	40.7	44.9	63.8	51.3	73.0	58.1
G_4T_4	A	43.2	43.3/42.8	61.4	73.8/67.6	NS	NS	95.0	NS	–	–
	E	–	–	60.5	65.6	–	–	–	–	–	–

[a]BC, biphasic curve; NS, nonsigmoidal curve, for which the enthalpy is not determined. ΔH_{vH} values obtained by CD/UV or by TGGE. The standard deviation of T_m is ±0.5 °C, and the ΔH_{vH} error is approximately ±5%. [b]Legend: 265 nm, P; 293 nm, A; TGGE, E. [c]With PEG 200 to a final concentration of 50%. [d]The second transition was analyzed.

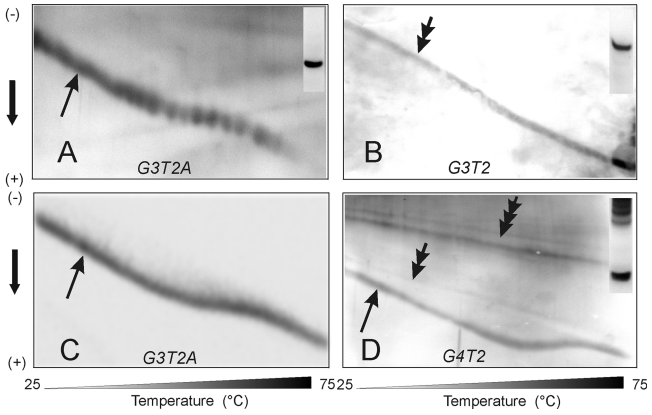

FIGURE 5: Representative TGGE records of the G_3T_2A oligomer in Britton-Robinsson buffer in 50 mM NaCl (A) or 50 mM KCl (B), G_3T_2 at 2.5 mM KCl (C), and G_4T_2 at 2.5 mM KCl (D). Insets in each panel depict the corresponding PAGE performed at 20 °C.

An objective melting curve obtained from electrophoretic records by ridge tracking analysis (Figure S7 of the Supporting Information) as applied for proteins has been used for this purpose (*22*). T_m values and van't Hoff enthalpy changes are summarized in Table 2.

The TGGE results clearly demonstrate that CD spectroscopy results are a convolution of several conformers of G-quadruplexes. Interestingly, parallel multimers marked with double arrows move faster after denaturation due to strand separation (Figure 5C), and intramolecular quadruplexes after denaturation move more slowly due to strand unfolding (Figure 5A,B,D).

This characteristic feature of mobility curves can be applied to the determination of the molecularity of quadruplex unfolding, and together with CD spectroscopy, it also allows for the evaluation of strand orientation, mainly for nonpolymorphic states.

DISCUSSION

Structural Polymorphism of Quadruplex Folding. There is currently tremendous interest in the understanding of G-quadruplex formation from G-rich sequences. These results demonstrate that all the G-rich sequences studied here tend to form quadruplexes. These results induce two main questions concerning these quadruplexes. (i) What are their relative stabilities, and do they adopt a parallel or an antiparallel topology? (ii) How does their molecularity depend on the type and concentration of monovalent ion? Antiparallel quadruplexes typically display a positive CD signal at ~295 nm, while parallel quadruplexes display a positive signal at ~265 nm. These differences reflect both the arrangements of the strands and the *syn* versus *anti* orientations around the glycosidic bonds. Parallel topologies have all-*anti* glycosidic angles, while the antiparallel ones have both *syn* and *anti* conformations in varying ratios (*43*). The complexes appear to be intramolecular rather than intermolecular (*37*). However, this is only valid for the sequences containing three or more bases between the neighboring G-runs and a lower concentration of potassium. The presence of smaller ions, Li^+ and Na^+, stabilizes intramolecular G-quadruplexes. Despite the fact that the electrophoretic separation of G-quadruplexes is performed in a polyacrylamide gel which partially induces mild crowding conditions, no significant changes in the quadruplex topology have been observed until the level of PEG 200 in the gel reached 20−50%. Electrophoresis in the presence of 30% PEG 200 confirms that the most preferred forms are parallel intramolecular/intermolecular conformations (Figure 1B−H and Figure S6 of the Supporting Information). It should be pointed out that we did not focus on quadruplex stability under crowding conditions, because 50% PEG 200 increases the thermal stability of G_3T_2A and G_3T_3 very significantly (Table 2). This observation is an agreement with the results of other authors (*33*, *44*). Nevertheless, PEG 200 plays a significant role not only in the thermal stability but also in the topology of G-quadruplexes (*31*, *33*, *34*).

Electrophoresis in a nondenaturing condition and CD spectra confirms that all sequences spontaneously form more than one

conformer in solution, although G_3T_2 seems to fold predominantly into intermolecular parallel conformers in the presence of 50−200 mM potassium.

However, we strongly believe that in nature there must be an existing factor forcing a quadruplex to fold into a more defined structure, similar to the way in which PEG mimics crowding conditions.

Thermal Stability. CD spectroscopy is an extremely useful method for studying a wide range of DNA conformational properties, but the structural conclusions must be treated with caution. It has been shown previously by other authors that the number of guanine residues in a G-cluster does not necessarily reflect the number of G-quartets present in a folded G-quadruplex (*16*). Our results, as well as those of other studies, show that it is more relevant to compare the number of G-tetrads in folded inter- and intramolecular structures. An oligonucleotide concentration used in CD, UV spectroscopy, and electrophoresis does not affect the melting temperature of G-quadruplexes (*28*, *29*, *36*). The thermodynamic evaluation of sequences G_3T_2, G_3T_4, and G_4T_2 has been performed by some other authors (*28*, *36*). Our results and conclusions agree with their data in most cases. We point out here that chemically modified oligomers are frequently used for thermal stability determination, and this modification can affect the population of multimeric structures. Some authors utilize the so-called FRET effect for thermodynamic evaluation, but fluorescently labeled oligomers may not allow analysis of all conformations occurring in solution during measurements.

In a recent review article, Chaires has tried to explain why spectroscopic thermodynamic data, T_m and enthalpy values, fall in an unacceptably wide range (*40*). Here, we show clearly that melting curves do not reflect the true transition of two-state melting of quadruplex structures, but only a mean value of the melting transitions of all conformers that are confirmed by electrophoresis as occurring in solution. However, the TGGE results are largely in agreement with the UV/CD measurements. Chaires' critical comments concerning data evaluation agree with our results. A set of spectra as a function of temperature defines a three-dimensional surface that can easily be converted to a matrix. Therefore, all the CD/UV spectra as a function of temperature have also been collected, rather than merely single-wavelength data (Figures S1 and S2 of the Supporting Information). An additional test of the two-state assumption can be provided within singular-value decomposition of the matrix to enumerate precisely the number of significant spectral species required to account for the spectral changes without reference to any specific model (*40*, *45*).

Topological Variability. In contrast, the *Tetrahymena* sequence $d(G_4T_2)_n$, which differs from the human sequence with an exchange of A for G in each repeat, could in principle generate four stacked G-quartets linked by two-base loops. Although this has been observed for the intermolecular dimer (*46*), the intramolecular complex instead folds to form only three quartets with variable loops consisting of TGGT, TTG, and TT (*47*). However, our results based on electrophoretic separation and spectral measurements show that at least one conformer of two intramolecular conformers exhibits a positive peak at 295 nm. The thermal stabilities of those monomers are different. However, the proportion of the less stable conformer is lower at higher temperatures, and perhaps at its proportion under the natural conditions of *Tetrahymenas*, it could be the dominant conformer. On the basis of this result, we suggest that this less stable conformer is intramolecular and that the second could consist of four G-tetrads. The band highlighted with an asterisk in Figure 2b disappeared when the electrophoretic separation was performed at 55 °C (Figure S4 of the Supporting Information).

In a comparison of these results with those published for sequences of the type $(G_3T_n)_4$, it is clear that adding G bases to the sequence has a different effect compared to the effect of adding extra T bases to the loops (*39*). $d(G_3T_3)_4$ and $d(G_4T_2)_4$ have the same repeat length, although the former adopts an antiparallel topology while the latter is largely parallel. The human $d(G_3T_2A)_4$ repeat also has the same repeat length, but it adopts an antiparallel hybrid topology in a solution containing K^+; there is also a small difference shown in Figure 2b.

It is known that intramolecular G-quadruplexes usually contain two to four G-tetrads; therefore, for the longer repeats, it is clear that a folded structure must contain some G residues in the loops (*21*, *28*). The amount of Na^+ and K^+ associated in quadruplex folding can indicate some trends concerning the number of stacked G-quartets in each complex, which are consistent with the gel mobility patterns (*29*). However, the calculation of the number of cations is based on the spectroscopic measurement, where several structures could be envisaged depending on which G bases are stacked and which are in the loops; several different forms may coexist in a solution in which the G-strands slip relative to each other.

Staining Procedure. During this research, we made use of the silver staining procedure. The sensitivity of this method is comparable to that of radioactive visualization (*23*). In addition, small populations of conformers can be detected, even though they are below the radioactive detection limit. This fact can be explained by the high affinity of silver and also by more efficient binding within highly ordered structures. Therefore, the intensity of low-molecular bands and the most abundant structures may not be proportional to their concentration. Nevertheless, the visualization with silver explains many facts that we can not explain without the presence of these conformers. We have also tested other staining procedures, for example, Stains-all and SYBR Green II fluorescent visualization of DNA in an electrophoretic gel, but we obtained significantly less sensitive staining which did not allow the detection of multimolecular structures.

Overall Conclusion. We have shown that G-quadruplex folding is a very sensitive molecular process and that the final topology depends on many factors. Interestingly, the *Tetrahymena* repeats seem to be more polymorphic, as is also the case with human telomeric repeats. In addition, we have shown that most G-rich repeats fold into topologically different conformers. Despite the fact that intermolecular folding is preferred under certain conditions for natural telomeric repeats, intermolecular conformers are always present under native conditions. Multiconformational states are one of the main reasons why such huge discrepancies between melting temperatures and enthalpy changes have been observed by other authors. The stabilization effect of the smallest lithium ion seems to be insufficient to stabilize a quadruplex structure under native conditions. Our analysis confirms that sodium and potassium ions have a relevant influence on structural stability within quadruplex folding.

SUPPORTING INFORMATION AVAILABLE

Supplementary analysis of CD measurements and electrophoresis (Figures S1−S8 and Table S1). This material is available free of charge via the Internet at http://pubs.acs.org.

REFERENCES

1. Grandin, N., and Charbonneau, M. (2008) Protection against chromosome degradation at the telomeres. *Biochimie 90*, 41–59.
2. McEachern, M. J., Krauskopf, A., and Blackburn, E. H. (2000) Telomeres and their control. *Annu. Rev. Genet. 34*, 331–358.
3. Londoño-Vallejo, J. A. (2008) Telomere instability and cancer. *Biochimie 90*, 73–82.
4. Phan, A. T., Kuryavyi, V., and Patel, D. J. (2006) DNA architecture: From G to Z. *Curr. Opin. Struct. Biol. 16*, 288–298.
5. Crnugelj, M., Sket, P., and Plavec, J. (2003) Small change in a G-rich sequence, a dramatic change in topology: New dimeric G-quadruplex folding motif with unique loop orientations. *J. Am. Chem. Soc. 125*, 7866–7871.
6. Blackburn, E. H. (1991) Structure and function of telomeres. *Nature 350*, 569–573.
7. Rhodes, D., and Giraldo, R. (1995) Telomere structure and function. *Curr. Opin. Struct. Biol. 5*, 311–322.
8. Wellinger, R. J., and Sen, D. (1997) The DNA structures at the ends of eukaryotic chromosomes. *Eur. J. Cancer 33*, 735–749.
9. Schaffitzel, C., Berger, I., Postberg, J., Hanes, J., Lipps, H. J., and Plückthun, A. (2001) In vitro generated antibodies specific for telomeric guanine-quadruplex DNA react with *Stylonychia lemnae* macronuclei. *Proc. Natl. Acad. Sci. U.S.A. 98*, 8572–8577.
10. Guo, Q., Lu, M., and Kallenbach, N. R. (1993) Effect of thymine tract length on the structure and stability of model telomeric sequences. *Biochemistry 32*, 3596–3603.
11. Hazel, P., Huppert, J., Balasubramanian, S., and Neidle, S. (2004) Loop-length-dependent folding of G-quadruplexes. *J. Am. Chem. Soc. 126*, 16405–16415.
12. Li, J., Correia, J. J., Wang, L., Trent, J. O., and Chaires, J. B. (2005) Not so crystal clear: The structure of the human telomere G-quadruplex in solution differs from that present in a crystal. *Nucleic Acids Res. 33*, 4649–4659.
13. Wang, Y., and Patel, D. J. (1993) Solution structure of the human telomeric repeat d[$AG_3(T_2AG_3)_3$] G-tetraplex. *Structure 1*, 263–282.
14. Parkinson, G. N., Lee, M. P., and Neidle, S. (2002) Crystal structure of parallel quadruplexes from human telomeric DNA. *Nature 417*, 876–880.
15. Dai, J., Carver, M., and Yang, D. (2008) Polymorphism of human telomeric quadruplex structures. *Biochimie 90*, 1172–1183.
16. Xu, Y., Noguchi, Y., and Sugiyama, H. (2006) The new models of the human telomere d[$AGGG(TTAGGG)_3$] in K^+ solution. *Bioorg. Med. Chem. 14*, 5584–5591.
17. Phan, A. T., Kuryavyi, V., Luu, K. N., and Patel, D. J. (2007) Structure of two intramolecular G-quadruplexes formed by natural human telomere sequences in K^+ solution. *Nucleic Acids Res. 35*, 6517–6525.
18. Luu, K. N., Phan, A. T., Kuryavyi, V., Lacroix, L., and Patel, D. J. (2006) Structure of the human telomere in K^+ solution: An intramolecular (3+1) G-quadruplex scaffold. *J. Am. Chem. Soc. 128*, 9963–9970.
19. Rujan, I. N., Meleney, J. C., and Bolton, P. H. (2005) Vertebrate telomere repeat DNAs favor external loop propeller quadruplex structures in the presence of high concentrations of potassium. *Nucleic Acids Res. 33*, 2022–2031.
20. Ambrus, A., Chen, D., Dai, J., Bialis, T., Jones, R. A., and Yang, D. (2006) Human telomeric sequence forms a hybrid-type intramolecular G-quadruplex structure with mixed parallel/antiparallel strands in potassium solution. *Nucleic Acids Res. 34*, 2723–2735.
21. Mergny, J. L., Phan, A. T., and Lacroix, L. (1998) Following G-quartet formation by UV-spectroscopy. *FEBS Lett. 435*, 74–78.
22. Víglaský, V., Antalík, M., Bagel'ová, J., Tomori, Z., and Podhradský, D. (2000) Heat-induced conformational transition of cytochrome c observed by temperature gradient gel electrophoresis at acidic pH. *Electrophoresis 21*, 850–858.
23. Bassam, B. J., and Gresshoff, P. M. (2007) Silver staining DNA in polyacrylamide gels. *Nat. Protoc. 2*, 2649–2654.
24. Viglasky, V. (2009) Platination of telomeric sequences and nuclease hypersensitive elements of human c-myc and PDGF-A promoters and their ability to form G-quadruplexes. *FEBS J. 276*, 401–409.
25. Vorlícková, M., Chládková, J., Kejnovská, I., Fialová, M., and Kypr, J. (2005) Guanine tetraplex topology of human telomere DNA is governed by the number of (TTAGGG) repeats. *Nucleic Acids Res. 33*, 5851–5860.
26. Kypr, J., Kejnovská, I., Renciuk, D., and Vorlíčková, M. (2009) Circular dichroism and conformational polymorphism of DNA. *Nucleic Acids Res. 37*, 1713–1725.
27. Gray, D. M., Wen, J. D., Gray, C. W., Repges, R., Repges, C., Raabe, G., and Fleischhauer, J. (2008) Measured and calculated CD spectra of G-quartets stacked with the same or opposite polarities. *Chirality 20*, 431–440.
28. Olsen, C. M., Lee, H. T., and Marky, L. A. (2009) Unfolding Thermodynamics of Intramolecular G-Quadruplexes: Base Sequence Contributions of the Loops. *J. Phys. Chem. B 113*, 2587–2595.
29. Rachwal, P. A., Brown, T., and Fox, K. R. (2007) Effect of G-tract length on the topology and stability of intramolecular DNA quadruplexes. *Biochemistry 46*, 3036–3044.
30. Fialová, M., Kypr, J., and Vorlícková, M. (2006) The thrombin binding aptamer GGTTGGTGTGGTTGG forms a bimolecular guanine tetraplen. *Biochem. Biophys. Res. Commun. 344*, 50–54.
31. Renciuk, D., Kejnovská, I., Skoláková, P., Bednárová, K., Motlová, J., and Vorlícková, M. (2009) Arrangements of human telomere DNA quadruplex in physiologically relevant K^+ solutions. *Nucleic Acids Res. 19*, 6625–6634.
32. Miyoshi, D., Nakao, A., and Sugimoto, N. (2003) Structural transition from antiparallel to parallel G-quadruplex of d($G_4T_4G_4$) induced by Ca^{2+}. *Nucleic Acids Res. 31*, 1156–1163.
33. Miyoshi, D., Nakao, A., and Sugimoto, N. (2002) Molecular crowding regulates the structural switch of the DNA G-quadruplex. *Biochemistry 41*, 15017–15024.
34. Miyoshi, D., and Sugimoto, N. (2008) Molecular crowding effects on structure and stability of DNA. *Biochimie 90*, 1040–1051.
35. Abu-Ghazalah, R. M., and Macgregor, R. B., Jr. (2009) Structural polymorphism of the four-repeat *Oxytricha nova* telomeric DNA sequences. *Biophys. Chem. 141*, 180–185.
36. Rachwal, P. A., Findlow, I. S., Werner, J. M., Brown, T., and Fox, K. R. (2007) Intramolecular DNA quadruplexes with different arrangements of short and long loops. *Nucleic Acids Res. 35*, 4214–4222.
37. Smargiasso, N., Rosu, F., Hsia, W., Colson, P., Baker, E. S., Bowers, M. T., DePauw, E., and Gabelica, V. (2008) G-quadruplex DNA assemblies: Loop length, cation identity, and multimer formation. *J. Am. Chem. Soc. 130*, 10208–10216.
38. Phan, A. T., Kuryavyi, V., Ma, J. B., Faure, A., Andréola, M. L., and Patel, D. J. (2005) An interlocked dimeric parallel-stranded DNA quadruplex: A potent inhibitor of HIV-1 integrase. *Proc. Natl. Acad. Sci. U.S.A. 102*, 634–639.
39. Lane, A. N., Chaires, J. B., Gray, R. D., and Trent, J. O. (2008) Stability and kinetics of G-quadruplex structures. *Nucleic Acids Res. 36*, 5482–5515.
40. Chaires, J. B. (2009) Human telomeric G-quadruplex: Thermodynamic and kinetic studies of telomeric quadruplex stability. *FEBS J.* (in press).
41. Kumar, N., and Maiti, S. (2008) A thermodynamic overview of naturally occurring intramolecular DNA quadruplexes. *Nucleic Acids Res. 36*, 5610–5622.
42. Phan, A. T., and Patel, D. J. (2003) Two-repeat human telomeric d(TAGGGTTAGGGT) sequence forms interconverting parallel and antiparallel G-quadruplexes in solution: Distinct topologies, thermodynamic properties, and folding/unfolding kinetics. *J. Am. Chem. Soc. 125*, 15021–15027.
43. Dapic, V., Abdomerovic, V., Marrington, R., Peberdy, J., Rodger, A., Trent, J. O., and Bates, P. J. (2003) Biophysical and biological properties of quadruplex oligodeoxyribonucleotides. *Nucleic Acids Res. 31*, 2097–2107.
44. Arora, A., and Maiti, S. (2009) Differential Biophysical Behavior of Human Telomeric RNA and DNA Quadruplex. *J. Phys. Chem. B 113*, 8784–8792.
45. Antonacci, C., Chaires, J. B., and Sheardy, R. D. (2007) Biophysical characterization of the human telomeric $(TTAGGG)_4$ repeat in a potassium solution. *Biochemistry 46*, 4654–4660.
46. Phan, A. T., Modi, Y. S., and Patel, D. J. (2004) Two-repeat *Tetrahymena* telomeric d(TGGGGTTGGGGT) sequence interconverts between asymmetric dimeric G-quadruplexes in solution. *J. Mol. Biol. 338*, 93–102.
47. Wang, Y., and Patel, D. J. (1994) Solution structure of the *Tetrahymena* telomeric repeat d(T_2G_4)$_4$ G-tetraplex. *Structure 2*, 1141–1156.